Published in final edited form as:
Exp Physiol. 2010 December ; 95(12): 1132–1144. doi:10.1113/expphysiol.2010.054700.

Altered ion transport by thyroid epithelia from *CFTR*$^{-/-}$ pigs suggests mechanisms for hypothyroidism in Cystic Fibrosis

Hui Li, **Suhasini Ganta**, and **Peying Fong**
Department of Anatomy and Physiology, Kansas State University College of Veterinary Medicine, Manhattan, KS 66506, USA

Abstract

Subclinical hypothyroidism has been linked to Cystic Fibrosis (CF), and the cystic fibrosis transmembrane conductance regulator (CFTR) shown to be expressed in the thyroid. The thyroid epithelium secretes Cl^- and absorbs Na^+ in response to cAMP. Chloride secretion may provide a counter-ion for the SLC26A4 (Pendrin)-mediated I^- secretion which is required for the first step of thyroid hormonogenesis, thyroglobulin iodination. In contrast, few models exist to explain a role for Na^+ absorption. Whether CFTR mediates the secretory Cl^- current in thyroid epithelium has not been directly addressed. We used thyroids from a novel pig *CFTR*$^{-/-}$ model, generated primary pig thyroid epithelial cell cultures (pThECs), analyzed these cultures for preservation of thyroid-specific transcripts and proteins, and monitored 1) the Cl^- secretory response to the cAMP agonist, isoproterenol and 2) the amiloride-sensitive Na^+ current. Baseline short-circuit current (I_{sc}) did not differ between *CFTR*$^{+/+}$ and *CFTR*$^{-/-}$ cultures. Serosal isoproterenol increased I_{sc} in *CFTR*$^{+/+}$, but not *CFTR*$^{-/-}$, monolayers. Compared to *CFTR*$^{+/+}$ thyroid cultures, amiloride-sensitive Na^+ absorption measured in *CFTR*$^{-/-}$ pThECs represented a greater fraction of the resting I_{sc}. However, levels of transcripts encoding ENaC subunits did not differ between *CFTR*$^{+/+}$ and *CFTR*$^{-/-}$ pThECs. Immunoblot analysis verified ENaC subunit protein expression, but quantification indicated no difference in expression levels. Our studies definitively demonstrate that CFTR mediates cAMP-stimulated Cl_- secretion in a well-differentiated thyroid culture model, and that knockout of *CFTR* promotes increased Na^+ absorption by a mechanism other than increased ENaC expression. These findings suggest several models for the mechanism of CF-associated hypothyroidism.

Keywords

CFTR; hypothyroidism; ion transport

Introduction

Cystic Fibrosis (CF) is a genetic disease that affects epithelial tissues of multiple organ systems, including the thyroid gland (Devuyst *et al.*, 1997; Welsh, 2001). It results from mutations in *CFTR*, the gene encoding the Cystic Fibrosis Transmembrane Conductance Regulator (Riordan *et al.*, 1989). The CFTR protein functions both as a Cl^- channel as well as a regulator of other important channels and transporters (Schwiebert *et al.*, 1999; Sheppard & Welsh, 1999). Recent studies suggest that this latter function depends critically on CFTR's participation within multi-molecular signaling complexes via specialized

Address correspondence to: Peying Fong, Ph.D., Department of Anatomy and Physiology, Kansas State University College of Veterinary Medicine, 1600 Denison Avenue, Manhattan, KS 66506, USA, Telephone: 785-532-4524, pfong@vet.k-state.edu.

protein-protein interactions, such as those facilitated by its regulatory (R) domain and its carboxyl terminal PDZ domain-binding motif (Ko *et al.*, 2004).

Increasing the overall quality of life markedly extends the median life expectancy for CF patients. Most studies of CF disease focus on its role in tissues in which overt and profound pathology has been found, resulting in significant mortality and morbidity. Other, subtler aspects of CF disease have been investigated less extensively. Small changes in thyroid hormone status impact on multiple organ systems during all stages of embryonic, early post-natal and adult life (Carrasco, 1993). Interestingly, subclinical hypothyroidism has been reported in CF patients (Madoff, 1968; De Luca *et al.*, 1982; Panesar, 1999), and CFTR has been localized subapically in bovine thyroid follicular epithelial cells (Devuyst *et al.*, 1997). Proper thyroid function has profound effects in multiple physiological processes, including the acquisition of hearing, regulation of cardiac function and metabolism (Klein & Danzi, 2007; Wangemann *et al.*, 2009; Liu & Brent, 2010). It therefore must be regarded in considerations of longevity and quality of life in CF patients.

Iodide is an essential component of the thyroid hormones, triiodothyronine (T_3) and thyroxine (T_4). Critical to thyroid function is the transport of I^- into the follicular lumen, where it is coupled to thyroglobulin to form the precursor to thyroid hormone (Carrasco, 1993). The avid uptake of I^- from the blood is mediated by the $Na^+ - I^-$ symporter, NIS, and its accumulation into the follicular lumen involves, at least partially, the product of the *SLC26A4* gene, Pendrin (Dai *et al.*, 1996; Everett *et al.*, 1999; Royaux *et al.*, 2000; Yoshida *et al.*, 2002). Pendrin is capable of transporting I^- in exchange for a variety of anions, including Cl^- (Scott *et al.*, 1999). Cyclic AMP-stimulated Cl^- secretion and channel activity have been measured in porcine thyrocytes, raising the possibility that this process provides the counter-ion for Pendrin-mediated I^- translocation (Champigny *et al.*, 1990; Armstrong *et al.*, 1992a; Armstrong *et al.*, 1992b; Bourke *et al.*, 1995). However, whether CFTR mediates apical Cl^- secretion in thyroid remains largely suggestive and unconfirmed. Pendrin activity may also be regulated by CFTR via interactions of its sulfate transporter anti-sigma factor antagonist (STAS) domain with CFTR's regulatory (R) domain (Gray, 2004; Ko *et al.*, 2004; Shcheynikov *et al.*, 2008).

Amiloride-sensitive Na^+ absorption presents strongly in primary thyroid epithelial cultures (Pearson *et al.*, 1988; Penel *et al.*, 1989), yet its role in thyroid function remains elusive and open to speculation. Single channel studies suggest that at least two different populations of Na^+ channels, including a low conductance channel that is highly sensitive to amiloride, underlie trans-follicular Na^+ absorption (Verrier *et al.*, 1989; Bourke *et al.*, 1996). The properties of the low-conductance channel suggest a classic ENaC assembly consisting of α-, β- and γ-ENaC subunits (Canessa *et al.*, 1994; Alvarez de la Rosa *et al.*, 2000). *In situ* hybridization studies showing the presence of ENaC mRNAs in mouse thyroid (Rochelle *et al.*, 2000) lend support to the notion that amiloride-sensitive Na^+ absorption is at least partially mediated by ENaC.

In addition to providing I^- for pro-hormone generation, thyroid ion transport may determine follicular volume and ionic composition, much in the same manner that it is believed to influence the airway surface liquid volume and composition. In airway surface epithelial cells, a large body of evidence points to a role of CFTR as a negative regulator of Na^+ transport; disruption of CFTR results in unabated Na^+ absorption (Mall *et al.*, 2004; Boucher, 2007b, c, a; Donaldson & Boucher, 2007). Ideally, an inquiry into the involvement of CFTR in thyroid transport mechanisms would compare absorption and secretion by thyroid epithelial monolayers in which *CFTR* is knocked out with the corresponding responses of thyroid epithelia derived from wild type controls. Several mouse models for CF are available but unfortunately they do not faithfully recapitulate many aspects of the human

disease (Grubb & Boucher, 1999; Scholte *et al.*, 2006). It stands to reason that relevance to human CF disease would best be achieved by using tissues from a model organism that bears physiological similarity to humans. In this respect, pig models have come into favor. Indeed, porcine physiology closely reflects that of humans, particularly the function of the cardiovascular, respiratory and gastrointestinal systems. This has been utilized to impressive effect in models of coronary artery disease and chronic ischemia (Hughes *et al.*, 2003). Recently developed porcine models for CF, $CFTR^{-/-}$ and transgenic pigs bearing the ΔF508 mutation, provide ideal and powerful models to conduct investigations of CFTR function (Rogers *et al.*, 2008a; Rogers *et al.*, 2008b). Importantly, the porcine model recapitulates many aspects of human CF disease (Rogers *et al.*, 2008a; Rogers *et al.*, 2008b; Stoltz *et al.*, 2010). The availability of these novel animals facilitates the present studies, which test whether the cAMP-mediated Cl^- secretory response previously measured in porcine thyroid cultures indeed is CFTR-mediated and whether Na^+ hyperabsorption extends to the thyroid (Armstrong *et al.*, 1992b).

We report herein a comparison of the 1) cAMP-stimulated Cl^- secretion and 2) amiloride-sensitive Na^+ absorption, measured in primary $CFTR^{+/+}$ and $CFTR^{-/-}$ pig thyroid epithelial monolayers as the short-circuit current (I_{sc}) in Ussing chambers. Comprehensive quantitative real-time reverse transcriptase polymerase chain reaction (qRT-PCR) and immunoblot analyses show the conservation of selected thyroid transporters, channels and enzymes, providing evidence for a high degree of differentiation in our pThEC cultures and lending molecular context for our functional findings.

Materials and Methods

Tissue procurement

Briefly, thyroid glands from newborn $CFTR^{+/+}$ and $CFTR^{-/-}$ piglets were surgically excised, transferred to cold Hank's Buffered Saline Solution (HBSS; Invitrogen, Carlsbad, CA) and shipped overnight on ice from the laboratory of Prof. Michael Welsh (HHMI, University of Iowa). Animals were euthanized in full compliance with protocols based on national guidelines and approved by the Institutional Animal Care and Use Committee at the University of Iowa. All Material Transfer Agreements between the Howard Hughes Medical Institutes at the University of Iowa and Kansas State University were executed before any tissue transfers were permitted.

Histology

Small blocks of thyroid tissue were trimmed of connective tissue and fixed in 4% paraformaldehyde before embedding in paraffin and sectioning. Hematoxylin and eosin (HE) staining was performed by the Histopathology service of the Kansas State Veterinary Diagnostic Lab. Samples were genotype-masked on submission to the service.

Preparation of primary cultures

Primary cultures of pig thyroid epithelial cells (pThECs) were prepared by adapting a method described for human thyroid culture (Williams & Wynford-Thomas, 1997). On receipt of thyroids from the Welsh lab, the glands were transferred into cold Hank's buffered Salt Solution (HBSS) and trimmed of connective tissue. The thyroids were washed in HBSS containing penicillin-streptomycin (HBSS/PS) and subsequently minced into small (~ 1 mm^3) pieces. The minced tissue was washed 3 times with HBSS/PS to remove blood cells, allowing settling by gravity between washes, before dissociation into follicles by sequential digestion using a Dissociation Medium (DM; HBSS containing 32 U/ml collagenase (type A; Roche, Indianapolis, IN) and dispase 1 mg/ml (grade II; Roche)). For neonatal thyroids, complete dissociation was achieved by digestion at 37 °C for ~1 h with vigorous shaking at

15 min intervals. Digestion was stopped by adding fetal bovine serum (FBS; Invitrogen) and follicles allowed to settle by gravity sedimentation on ice for 1 h. The supernatant was carefully removed from the loose pellets and discarded. Pellets were resuspended in fresh Dulbecco's Modified Eagles Medium (DMEM; Invitrogen), then pooled and rinsed 3X by centrifugation for 5 min at 200 × g. The resultant pellets were resuspended in 2–5 mL growth medium (GM; DMEM with 10% FBS, penicillin/streptomycin and TSH (0.1 IU/mL; Sigma Chemical Company, St. Louis, MO)) and passed through a 100 μm mesh cell strainer. The follicle suspension was seeded on permeable growth supports (Snapwell #3407 and Transwell #3412; Costar Corning). Cells were maintained in a humidified, 37°C, 5% CO_2 incubator. In addition, cells were seeded on T25 flasks to allow visual assessment of growth pattern and morphology. GM was changed one day post-seeding and biweekly thereafter. Cells could be passaged once without significant alteration of transport properties.

Measurements of short-circuit Current (I_{sc})

Epithelial monolayers cultured from $CFTR^{+/+}$ and $CFTR^{-/-}$ thyroids were measured at ~ 2 weeks (13–16 days) post-seeding, when transepithelial resistance (R_{te}) achieved mean values exceeding 1 kΩ · cm^2. Briefly, Snapwell supports were mounted on modified bicameral chambers (model CHM-5, WPI, Sarasota, FL) connected to water-jacketed glass reservoirs maintained at 37 °C. Electrodes for measuring the transepithelial voltage (V_{te}) and passing current (I) consisted of AgCl pellets embedded in a matrix consisting of 1% agar/1 M KCl. Both sets of electrodes were connected to an epithelial voltage clamp amplifier (model EC-825; Warner Instruments, Hamden, CT), which in turn were interfaced with an iWorx 118 AD/DA device (iWorx; Concord, New Hampshire) to a laptop PC computer. Data were recorded using LabScribe 2 software (iWorx), with an acquisition rate of 1 sample per second. Each chamber was filled with Hepes-buffered mammalian Ringer's solution (HMR; *in mM*, 140 NaCl, 2.7 KCl, 1.8 $CaCl_2$, 1.06 $MgCl_2$, 12.4 Hepes, 5.1 glucose, pH 7.4 with NaOH). Both mucosal and serosal solutions were bubbled continuously with room air. After stabilization of transepithelial voltage (V_{te}) and notation of the transepithelial resistance (R_{te}), the tissues were voltage clamped and I_{sc} was recorded continuously. Isoproterenol and amiloride (Sigma) were added from 10^{-2} M (1000X) aqueous stocks, and forskolin (also from Sigma) added from a 1000× DMSO stock.

Quantitative RT-PCR

Total RNA was isolated from confluent pThECs at 2 weeks post-seeding (RNeasy Mini kit; Qiagen, Valencia, CA) and treated with on-column RNase-free DNase I (Qiagen). Total RNA was quantified using absorption spectrophotometry (Nanodrop 8000; Thermo Scientific, Wilmington, DE). The quality of total RNA samples was evaluated with RNA Nano LabChip on a 2100 Bioanalyzer (Agilent Technologies, Santa Clara, CA). Only RNA samples of high quality were subjected to quantitative RT-PCR (QuantiTect SYBR Green RT-PCR kit; Qiagen, Valencia, CA) in a 96-well plate format (iCycler, BioRad, Hercules, CA). Each reaction contained 100 ng of RNA and 0.5 μM of porcine gene-specific primer pairs (see Table 1). Primer pairs for *SCNN1A*, *SCNN1B* and *SCNN1G* (encoding α-, β-, γ-ENaC) and *SLC26A4* (encoding Pendrin) were published previously (Carlin *et al.*, 2006), as were primer pairs for NIS and 18S (Tedelind *et al.*, 2006). Primer pairs for porcine *CLCN5* and *CFTR* were based on NCBI Reference Sequences NM_214139.1 and NM_001104950.1, respectively. Expression of the gene encoding the cyclic nucleotide-gated cation channel, *CNGA1*, was probed using primer pairs based on cDNA sequences from Pig Genomic Informatics System (http://pig.genomics.org.cn/). Primers were designed using primer designing tool- NCBI/Primer-BLAST (http://www.ncbi.nlm.nih.gov/tools/primer-blast/). Table 1 summarizes primer sequences, expected product sizes and sequence accession numbers. All RT-PCR reactions consisted of RT for 30 min at 50°C and heating to 95°C for

15 min, followed by 40 PCR cycles of 30 s denaturation at 94°C, 30 s annealing at 58°C, 30 s elongation at 72°C, 15 s detection at 75°C and concluding with 30 s melting-curve analysis. RT-PCR products were analysed by gel electrophoresis and product identities confirmed by sequencing. The original fluorescence data were converted into initial reporter fluorescence (R_0) by using the DART-PCR (data analysis for real-time PCR) program (http://nar.oxfordjournals.org/cgi/content/full/31/14/e73/DC1) and adjusting for PCR efficiency differences (Peirson *et al.*, 2003;Cikos *et al.*, 2007). The relative gene expression levels were normalized to 18S R_0 values.

Immunoblotting

Confluent pThEC monolayers at ~ 2 weeks post-seeding were placed on ice and the growth medium removed before washing 3 times with phosphate buffered saline (PBS) and lysis in a buffer composed of (in mM) 150 NaCl, 50 Tris-HCl, 1% NP-40, 0.5% sodium dodecyl sulfate, pH 7.4 plus Complete™ protease inhibitor cocktail (Roche, Indianapolis, IN). After 5 minutes, the lysed cells were scraped. The lysates were collected, incubated for 30 min on ice and centrifuged at 13,000 rpm for 15 min at 4 °C. The supernatant fractions were collected and quantified by bicinchoninic acid assay (Thermo Scientific Pierce, Rockford, IL). Prior to gel electrophoresis, Laemmli buffer (containing 5% β-mercaptoethanol) was added to lysates (~ 20 μg each) and the samples were denatured at 37 °C for 30 min. Separated proteins were transferred to PVDF membrane and blocked for 1 h in 5% nonfat dry milk/Tris-buffered saline plus 0.1% Tween-20 (TBST). Primary antibody binding was performed overnight at 4 °C, followed by room temperature washes with TBST and horseradish peroxidase (HRP)-labeled secondary antibody binding for < 1 h at room temperature. After extensive washing (> 1 h) with TBST, SuperSignal Femto West substrate (Thermo Scientific Pierce) was applied and the resultant chemiluminescence acquired for densitometry (Image Station 4000R; Kodak, Rochester, NY). Densitometric data were normalized to the corresponding actin signals.

Antibodies

Rabbit polyclonal antibodies directed against rat α-, β- and γ-ENaC were the generous gifts of Prof. Cecilia Canessa (Yale University School of Medicine); early studies used antibodies from Mark Knepper (NHLBI) (Masilamani *et al.*, 1999). Rabbit polyclonal anti-ClC-5 was kindly provided by Prof. Thomas Jentsch (FMP Leibniz-Institut für Molekulare Pharmacologie, Berlin, FRG). Goat polyclonal antibodies against the Na^+-I^- symporter (NIS; P-14), dual oxidase 1 (DUOX1; S-18), thyroperoxidase (TPO; C-20) and thyroglobulin (Tg; N-15) were purchased from Santa Cruz Biotechnology. We used a mouse monoclonal antibody directed against the Na^+/K^+ ATPase α1 subunit (clone 464.6; Novus Biologicals, Littleton, CO). Mouse monoclonal anti-CFTR antibody 660, generated against a region of the human CFTR NBD1 (Cui *et al.*, 2007), was obtained from Cystic Fibrosis Foundation Therapeutics. Mouse monoclonal anti-actin was purchased from Millipore (Billerica, MA). Secondary antibodies used in these studies were HRP-labeled goat anti-mouse, donkey anti-goat secondary antibodies (both from Santa Cruz Biotechnology) and donkey anti-rabbit secondary antibodies (GE Amersham).

Statistical Analysis

Data are presented as mean values ± SEM. All comparisons were drawn between tissues derived from littermates unless otherwise specified. Statistical significance was evaluated by Student's *t*-test, with significance assigned at $p < 0.05$.

Results

CFTR$^{+/+}$ and CFTR$^{-/-}$ thyroid glands and pThECs show no obvious differences in histology or growth pattern

Thyroids from neonatal pigs comprise two fused lobes and showed variability in overall morphology; this variation did not correlate with genotype. HE staining of fixed tissue sections prepared from *CFTR*$^{+/+}$ and *CFTR*$^{-/-}$ thyroids next was performed to determine if gene disruption altered tissue morphology. Figure 1A shows the follicular organization of cuboidal epithelial cells characteristic of the thyroid gland. No obvious differences (follicle size, number, gross cellular morphology) can be noted between the wild type (*left panel*) and knockout (*right panel*) sections. Thus, ablation of the *CFTR* gene does not disrupt the thyroid follicular structure. We next evaluated whether the lack of functional CFTR influenced how primary follicular cultures grew. After one week of growth on plastic, there were no differences between the *CFTR*$^{+/+}$ and *CFTR*$^{-/-}$ cultures (fig. 1B; *compare left and right panels*), which form confluent monolayers indistinguishable in overall appearance on the light microscopic level.

Expression of mRNA encoding known thyroid transporters by CFTR$^{+/+}$ and CFTR$^{-/-}$ pThECs

To determine whether transport proteins expressed by thyroid follicular epithelial cells are preserved in our primary culture model, we performed qRT-PCR using primers specific for *CFTR*, *SLC5A5* (encoding the sodium-iodide symporter, NIS), *CLCN5* (encoding ClC-5, a Cl^-/H^+ antiporter that, when knocked out in a mouse model, associates with euthyroid goiter; (van den Hove *et al.*, 2006)) and *SLC26A4* (Pendrin) (*see* Table 1). Amplification with pig *CFTR*-specific primers also served to confirm sample identity. Levels of *SLC5A5* and *CLCN5* transcript did not significantly differ between the *CFTR*$^{+/+}$ and *CFTR*$^{-/-}$ samples (*see* Table 2). However, efforts to detect *SLC26A4* transcript in the same samples yielded C_t values exceeding 35, beyond the limits of reliable qRT-PCR detection.

Thyroid-specific protein expression is conserved in pThEC cells

Immunoblot analysis was next performed to confirm expression of NIS and ClC-5. Figure 2 shows the results obtained for three pairs of litter-matched *CFTR*$^{+/+}$ *and CFTR*$^{-/-}$ pThEC cultures. NIS migrates as multiple glycosylated species (Levy *et al.*, 1998); in pThEC these run at ~73 (fig. 2A) and ~100 kDa (fig. 2B). In mouse thyroid, ClC-5 runs as a broad, major band at ~ 90 kDa, with a weaker band at ~80 kDa (van den Hove *et al.*, 2006). Both the 90 kDa band (fig. 2C), as well as faint levels of the 80 kDa species (*not shown*) are detected in *CFTR* $^{+/+}$ and *CFTR*$^{-/-}$ pThEC cells. The summarized densitometric quantification revealed no detectable difference in the wild type and knockout thyroid cells of either NIS band, as well as the 90 kDa ClC-5 band (fig. 2A–C). In addition, immunoblot analysis confirmed that 1) thyroglobulin, 2) dual oxidase (DUOX; the enzyme critical for generating hydrogen peroxide which is needed for thyroid I^- organification) and 3) thyroperoxidase (TPO, which catalyses the coupling of I^- to thyroglobulin) expression are preserved in the *CFTR*$^{+/+}$ and the *CFTR*$^{-/-}$ pThEC cultures (fig. 2E–G). Densitometry found no appreciable difference in either DUOX or TPO levels (fig. 2F and G). Thyroglobulin expression was consistently greater in lysates isolated from *CFTR*$^{-/-}$ pThECs, but this trend did not achieve significance (fig. 2E). Levels of the Na^+/K^+ ATPase did not differ between the sample sets (fig. 2H).

Resting and cAMP-agonist-stimulated bioelectric properties of CFTR$^{+/+}$ and CFTR$^{-/-}$ pThECs

After 2 weeks of primary culture, *CFTR*$^{+/+}$ and *CFTR*$^{-/-}$ pThECs formed electrically tight monolayers. Wild type and knockout pThECs did not exhibit obvious differences in

morphology. $CFTR^{+/+}$ monolayers gave initial R_{te} values of 3052 ± 776 Ω. cm^2 (n = 10 monolayers from 5 different tissue preparations, derived from 5 litters). Monolayers derived from litter-matched $CFTR^{-/-}$ thyroids produced R_{te} values of 4133 ± 568 Ω.cm^2 (n = 9 monolayers). The tendency toward higher R_{te} in $CFTR^{-/-}$ thyroids did not achieve significance. These findings contrast with observations that loss of CFTR function compromises junctional permeability in human bronchial epithelial cells (LeSimple *et al.*, 2010). Baseline I_{sc} values of $CFTR^{+/+}$ and $CFTR^{-/-}$pThECs likewise did not differ significantly. Wild type tissues produced 4.6 ± 0.93 μA (n = 10), whereas knockouts gave 4.9 ± 0.52 μA (n = 9; $p > 0.05$). Like airway epithelial monolayers, thyroid epithelial cultures transport bidirectionally, so mucosal amiloride (amil, 10^{-5} M) treatment prior to the delivery of cAMP agonist typically is performed in order to hyperpolarize the apical membrane, thereby maximizing the secretory Cl^- current. Serosal isoproterenol (iso, 10^{-5} M) stimulated I_{sc} in $CFTR^{+/+}$ monolayers, producing a transient increase (4.5 ± 1.17 μA; n = 9 monolayers from 5 preparations; fig. 3A, *iso*) before stabilization at a level higher than pre-iso treatment. These observations are qualitatively consistent with previous studies on primary cultures of adult pig thyroid, using prostaglandin E2 as the cAMP agonist (Armstrong *et al.*, 1992b). Forskolin (10 μM, serosal) produced similar effects (*data not shown*). In stark contrast, $CFTR^{-/-}$ pThECs did not increase I_{sc} in response to isoproterenol, but did occasionally produce a slight depression of I_{sc} (−0.3 ± 0.09 μA; n = 5 monolayers from 3 preparations; fig. 3B). Figure 3C summarizes the difference in the isoproterenol-mediated I_{sc} responses. These results demonstrate unequivocally that CFTR is necessary for mediating the cAMP-activated I_{sc} response in primary thyroid monolayers.

Compared to primary $CFTR^{+/+}$ pThECs, amiloride-sensitive I_{sc} is increased in cultures derived from $CFTR^{-/-}$ pigs

Recall that amiloride-sensitive absorption of Na^+ previously has been observed in adult pig thyroid cultures (Penel *et al.*, 1989). The present study shows that this property is preserved in cultured neonatal pThECs. Addition of amiloride (10^{-5} M) to the mucosal chamber inhibited I_{sc} in $CFTR^{+/+}$ and $CFTR^{-/-}$ cultures (fig. 3A and B, *amil*). Importantly, amiloride inhibited the I_{sc} to a significantly greater extent in primary cultures grown from $CFTR^{-/-}$ thyroids (fig. 3D; $p < 0.05$; n = 7 $CFTR^{+/+}$ and n = 5 $CFTR^{-/-}$ monolayers; 3 pairs of thyroids from 3 distinct litters). These findings are similar to observations made in airway surface epithelial cultures (Boucher *et al.*, 1988), also bi-directionally transporting epithelia, but differ from conclusions drawn from studies of the absorptive sweat duct (Reddy *et al.*, 1999).

$CFTR^{+/+}$ and $CFTR^{-/-}$ pThECs show similar levels of SCNN1A, SCNN1B and SCNN1G transcripts, as well as α-, β- and γ-ENaC subunit proteins

To test whether increased transcription of the genes encoding ENaC subunits underlies the increase in amiloride-sensitive I_{sc} (I_{sc}, *amil*), qRT-PCR studies were performed using primers previously shown to amplify porcine ENaC mRNA (*SCNN1A*, *SCNN1B* and *SCNN1G*; Table 1; (Carlin *et al.*, 2006)). As summarized in Table 2, *SCNN1A*, *SCNN1B* and *SCNN1G* were detected at similar levels in samples isolated from $CFTR^{+/+}$ and $CFTR^{-/-}$ cultures.

Modulation of total ENaC protein levels represents another level at which I_{sc}, *amil* could be regulated. To evaluate this possibility, we performed quantitative immunoblot analysis on total cell lysates of $CFTR^{+/+}$ and $CFTR^{-/-}$ pThECs. Figure 4 compares total ENaC subunit protein expression in cultures prepared from three litter-matched pairs of wild type and knockout thyroids. The corresponding blots probing for CFTR and actin are shown for comparision (fig. 4E). CFFT antibody 660, directed against residues 484–589 of human CFTR bearing 100% identity in pig CFTR, yields a broad, diffuse band at ~170 kDa with

total lysates prepared from $CFTR^{+/+}$ pThECs that was not present in the samples prepared from $CFTR^{-/-}$ pThECs (fig. 4E). This band corresponds to mature C band. The immature B band was not detected in $CFTR^{+/+}$ pThECs. Samples quantified with reference to actin levels showed insignificant differences in α-, β- and γ-ENaC subunits (fig. 4A–D). Levels of neither the full-length band of α-ENaC (~95 kDa) nor the amino-terminus cleavage fragment (~32 kDa) differed significantly between the $CFTR^{+/+}$ and $CFTR^{-/-}$ samples. This was also the case for β-ENaC (90 kDa)and γ-ENaC (83 kDa). These data argue against the notion that the lack of CFTR augments I_{sc}, *amil* through increased ENaC expression.

Discussion

Subclinical hypothyroidism has been linked to Cystic Fibrosis (CF) disease (Madoff, 1968; Panesar, 1999). Inadequate thyroid hormone levels profoundly affect a wide range of physiological processes, notably impairing cardiac contractility and decreasing metabolic rate. However, the mechanism whereby the lack of functional CFTR results in the hypothyroid state is poorly understood.

Early studies using primary cultures of thyroid epithelium demonstrated that this tissue, like airway surface epithelia, bi-directionally transports ions, secreting anions such as Cl^-, HCO_3^- and $I^{-/-}$ in response to cAMP agonists, as well as absorbing Na^+ (Bourke *et al.*, 1987; Nilsson *et al.*, 1990; Armstrong *et al.*, 1992a; Armstrong *et al.*, 1992b; Nilsson *et al.*, 1992). Previous single channel patch clamp measurements of thyroid follicular cells showed cAMP-dependent $Cl^{-/-}$ channel activity (Champigny *et al.*, 1990; Bourke *et al.*, 1995), with physiological and biophysical profiles fitting that of CFTR (Gray *et al.*, 1989; Sheppard & Welsh, 1999). Importantly, CFTR conducts $I^{-/-}$, a property relevant to thyroid function (Tabcharani *et al.*, 1992; Tabcharani *et al.*, 1997). Moreover, variations in halide permeability exist between orthologs. Opossum CFTR selects for $Cl^{-/-}$ over $I^{-/-}$ whereas the reverse exists for *Xenopus* CFTR (Price *et al.*, 1996; Demmers *et al.*, 2010). The overall similarities between pig and human CFTR make it tempting to surmise that relative anion permeability of porcine CFTR is identical to that of human CFTR. However, this remains to be demonstrated formally and indeed major functional differences between pig and human CFTR already have been found (Ostedgaard *et al.*, 2007; Liu *et al.*, 2008). Previous immunoblot, immunofluorescence and histochemical analyzes using rabbit polyclonal anti-CFTR antibodies demonstrated the presence of CFTR in subapical compartments of bovine thyroid epithelium (Devuyst *et al.*, 1997), but did not link these observations with functional measurements. CFTR expression was not uniform, but limited to select cells within follicles. Moreover, Devuyst *et al* noted a correlation between follicle size and the frequency of CFTR-positive cells, suggesting a relationship between follicular epithelial ion transport, the synthesis, storage and uptake of thyroglobulin and ultimately thyroid hormone status. Taken together, however, these observations led to an early hypothesis that CFTR may directly mediate at least a component of $I^{-/-}$ efflux from the thyrocyte and into the luminal space of the follicle (fig. 5A, *left*). Thus, one means by which CF-associated subclinical hypothyroidism may arise is based on a simple model whereby direct CFTR-mediated apical $I^{-/-}$ efflux is attenuated or ablated, depending on the mutation(s) carried (fig. 5B, *left*). The establishment of the $CFTR^{-/-}$ cultures enables future studies testing the impact of *CFTR* ablation on transepithelial $I^{-/-}$ fluxes at the very low physiological levels of basolateral/blood $I^{-/-}$.

More recent studies point to the importance of SLC26A4 in direct movement of $I^{-/-}$ during the process of follicular accumulation. Protein-protein interactions between CFTR and sulfate-transporter family members (such as SLC26A4) thus also may determine thyroid $I^{-/-}$ transport (fig. 5A, *middle*). The lack of functional CFTR could disrupt these interactions, thereby impairing follicular $I^{-/-}$ accumulation (fig. 5B, *middle*). In such a

model, CFTR *indirectly* mediates $I^{-/-}$ movement by virtue of regulatory interactions with SLC26A4. The present observations indicate that cAMP-activated $CI^{-/-}$ secretion is diminished in the CF thyroid, and thereby possibly disrupts this mechanism of $I^{-/-}$ accumulation. However, our findings do not exclude the possibility that CFTR mediates $I^{-/-}$ efflux directly nor do they rule out the possibility that these mechanisms coexist. Our qRT-PCR and immunoblot analyses show that many of the molecular players important in thyroid follicular epithelial function are preserved in our primary cultures. The apparent lack of SLC26A4 expression in both the wild type and knockout preparations confounds immediate experiments on our primary culture system that handily distinguish between these two models. Primers specific for the porcine SLC26A4 are limited, since the pig ortholog has yet to be completely cloned. We have screened many antibodies from commercial sources, as well as those received as gifts from multiple laboratories, but all have proven to be unsuitable for detection of the porcine SLC26A4/Pendrin. Our preliminary observation that P1 cultures maintain the same transport properties as the primary pThECs leaves open, as a possible future strategy, evaluation of anion transport following delivery and expression of SLC26A4.

The lack of functional CFTR has been associated with Na^+ hyperabsorption in airway epithelia, prompting us to test whether this would extend to thyroid follicular epithelial cells. Indeed, the increased $I_{sc,\,amil}$ measured in pThECs supports this notion. These findings suggest a third possibility: increased amiloride-sensitive Na^+ absorption may impede NIS-mediated $I^{-/-}$ accumulation (*compare* fig 5A and 5B, *right*). It is tempting to speculate that apical Na^+ absorption may compete with NIS-mediated Na^+ influx for the inward Na^+ gradient. NIS has a stoichiometry of $2Na^+$: 1 $I^{-/-}$, and thus like ENaC also carries a net inward positive charge in the form of Na^+ (Eskandari *et al.*, 1997; De La Vieja *et al.*, 2000). The predicted outcome of increased ENaC-mediated, apical Na^+ entry would be impairment of NIS-mediated I^- uptake, leading to diminished efficiency of thyroglobulin iodination and hormonogenesis.

The cellular mechanisms underlying the increased $I_{sc,\,amil}$ remain unclear. Relative expression of ENaC subunits in $CFTR^{+/+}$ and $CFTR^{-/-}$ pig thyroid primary cultures assessed by qRT-PCR measurements did not differ significantly for all three ENaCs. This finding is consistent with previous studies of freshly excised airway epithelia from CF and normal patients which show no difference in the mRNA levels of all three ENaC subunits (Burch *et al.*, 1995). We also examined levels of *CNGA1* transcript (Qiu *et al.*, 2000). Transcript encoding this cyclic nucleotide-gated channel, a non-selective cation channel that also is inhibited by amiloride, likewise did not differ (*see* Table 2). Subsequent immunoblot comparisons of ENaC subunit protein levels also showed no difference between the $CFTR^{+/+}$ and $CFTR^{-/-}$ thyroid groups. Proteolytic cleavage of ENaC recently has emerged as an important means of upregulating ENaC activity (Kleyman *et al.*, 2009). However, in our studies the observed increase in $I_{sc,\,amil}$ cannot be readily explained by increased proteolytic cleavage-based channel activation; the 32 kDa fragment of α-ENaC subunit did not increase in $CFTR^{-/-}$ thyroid and we were unable to detect γ-ENaC cleavage product with the antibodies used. Thus, although the overall $I_{sc,\,amil}$ increased, our data indicate that this functional difference cannot be accounted for by increased total ENaC subunit expression. However, they do leave open the possibility that ENaC surface expression/turnover is altered in $CFTR^{-/-}$ pThECs, forming the basis of future studies. Alternatively, these data are consistent with the notion that enhanced Na^+ absorption in $CFTR^{-/-}$ epithelia results from membrane hyperpolarization that is consequential to the lack of anion conductance.

In conclusion, we have shown preservation of proteins important to vectorial ion transport and thyroid function in primary thyroid cultures prepared from a novel porcine $CFTR^{-/-}$

model. The bidirectional transport properties of the cultures derived from the wild type neonatal thyroids resemble those reported previously for cultures derived from adult (wild type) pig thyroids. Using litter-matched cultures of *CFTR*$^{-/-}$ thyroids, our findings show definitively that cAMP-stimulated Cl^- secretion is mediated by CFTR in the thyroid, and that its loss promotes increased Na^+ absorption. Both of these disruptions in ion transport bear potentially significant implications for thyroid function and may contribute to the basic mechanisms underlying subclinical hypothyroidism in Cystic Fibrosis.

Acknowledgments

We are indebted to Prof. Michael J. Welsh and Dr. Phil Karp (HHMI, University of Iowa) for providing the pig thyroid glands. We thank Cystic Fibrosis Foundation Therapeutics for providing anti-CFTR, Prof. Thomas Jentsch for anti-ClC-5, as well as Prof. Cecilia Canessa and Dr. Mark Knepper for anti-ENaC antibodies. Support from NIH (COBRE NIH-P20-RR017686; Project 2 and Core C), and Kansas State University College of Veterinary Medicine (SUCCESS-FYI) is acknowledged gratefully.

References

Alvarez de la Rosa D, Canessa CM, Fyfe GK, Zhang P. Structure and regulation of amiloride-sensitive sodium channels. Annu Rev Physiol. 2000; 62:573–594. [PubMed: 10845103]

Armstrong J, Matainaho T, Cragoe EJ Jr, Huxham GJ, Bourke JR, Manley SW. Bidirectional ion transport in thyroid: secretion of anions by monolayer cultures that absorb sodium. Am J Physiol. 1992a; 262:E40–E45. [PubMed: 1733249]

Armstrong JW, Cragoe EJ Jr, Bourke JR, Huxham GJ, Manley SW. Chloride conductance of apical membrane in cultured porcine thyroid cells activated by cyclic AMP. Mol Cell Endocrinol. 1992b; 88:105–110. [PubMed: 1334005]

Boucher RC. Airway surface dehydration in cystic fibrosis: pathogenesis and therapy. Annu Rev Med. 2007a; 58:157–170. [PubMed: 17217330]

Boucher RC. Cystic fibrosis: a disease of vulnerability to airway surface dehydration. Trends Mol Med. 2007b; 13:231–240. [PubMed: 17524805]

Boucher RC. Evidence for airway surface dehydration as the initiating event in CF airway disease. J Intern Med. 2007c; 261:5–16. [PubMed: 17222164]

Boucher RC, Cotton CU, Gatzy JT, Knowles MR, Yankaskas JR. Evidence for reduced Cl- and increased Na+ permeability in cystic fibrosis human primary cell cultures. J Physiol. 1988; 405:77–103. [PubMed: 3255805]

Bourke JR, Abel KC, Huxham GJ, Sand O, Manley SW. Sodium channel heterogeneity in the apical membrane of porcine thyroid epithelial cells. J Endocrinol. 1996; 149:101–108. [PubMed: 8676041]

Bourke JR, Matainaho T, Huxham GJ, Manley SW. Cyclic AMP-stimulated fluid transport in the thyroid: influence of thyroid stimulators, amiloride and acetazolamide on the dynamics of domes in monolayer cultures of porcine thyroid cells. J Endocrino. 1987; 115:19–26.

Bourke JR, Sand O, Abel KC, Huxham GJ, Manley SW. Chloride channels in the apical membrane of thyroid epithelial cells are regulated by cyclic AMP. J Endocrinol. 1995; 147:441–448. [PubMed: 8543914]

Burch LH, Talbot CR, Knowles MR, Canessa CM, Rossier BC, Boucher RC. Relative expression of the human epithelial Na+ channel subunits in normal and cystic fibrosis airways. Am J Physiol. 1995; 269:C511–C518. [PubMed: 7653534]

Canessa CM, Schild L, Buell G, Thorens B, Gautschi I, Horisberger JD, Rossier BC. Amiloride-sensitive epithelial Na+ channel is made of three homologous subunits. Nature. 1994; 367:463–467. [PubMed: 8107805]

Carlin RW, Sedlacek RL, Quesnell RR, Pierucci-Alves F, Grieger DM, Schultz BD. PVD9902, a porcine vas deferens epithelial cell line that exhibits neurotransmitter-stimulated anion secretion and expresses numerous HCO3(-) transporters. Am J Physiol Cell Physiol. 2006; 290:C1560–C1571. [PubMed: 16421205]

Carrasco N. Iodide transport in the thyroid gland. Biochim Biophys Acta. 1993; 1154:65–82. [PubMed: 8507647]

Champigny G, Verrier B, Gerard C, Mauchamp J, Lazdunski M. Small conductance chloride channels in the apical membrane of thyroid cells. FEBS Lett. 1990; 259:263–268. [PubMed: 1688416]

Cikos S, Bukovska A, Koppel J. Relative quantification of mRNA: comparison of methods currently used for real-time PCR data analysis. BMC Mol Biol. 2007; 8:113. [PubMed: 18093344]

Cui L, Aleksandrov L, Chang XB, Hou YX, He L, Hegedus T, Gentzsch M, Aleksandrov A, Balch WE, Riordan JR. Domain interdependence in the biosynthetic assembly of CFTR. J Mol Biol. 2007; 365:981–994. [PubMed: 17113596]

Dai G, Levy O, Carrasco N. Cloning and characterization of the thyroid iodide transporter. Nature. 1996; 379:458–460. [PubMed: 8559252]

De La Vieja A, Dohan O, Levy O, Carrasco N. Molecular analysis of the sodium/iodide symporter: impact on thyroid and extrathyroid pathophysiology. Physiol Rev. 2000; 80:1083–1105. [PubMed: 10893432]

De Luca F, Trimarchi F, Sferlazzas C, Benvenga S, Costante G, Mami C, Di Pasquale G, Magazzu G. Thyroid function in children with cystic fibrosis. Eur J Pediatr. 1982; 138:327–330. [PubMed: 6813123]

Demmers KJ, Carter D, Fan S, Mao P, Maqbool NJ, McLeod BJ, Bartolo R, Butt AG. Molecular and functional characterization of the cystic fibrosis transmembrane conductance regulator from the Australian common brushtail possum, Trichosurus vulpecula. J Comp Physiol B. 2010; 180:545–561. [PubMed: 20012660]

Devuyst O, Golstein PE, Sanches MV, Piontek K, Wilson PD, Guggino WB, Dumont JE, Beauwens R. Expression of CFTR in human and bovine thyroid epithelium. Am J Physiol. 1997; 272:C1299–C1308. [PubMed: 9142856]

Donaldson SH, Boucher RC. Sodium channels and cystic fibrosis. Chest. 2007; 132:1631–1636. [PubMed: 17998363]

Eskandari S, Loo DD, Dai G, Levy O, Wright EM, Carrasco N. Thyroid Na+/I− symporter. Mechanism, stoichiometry, and specificity. J Biol Chem. 1997; 272:27230–27238. [PubMed: 9341168]

Everett LA, Morsli H, Wu DK, Green ED. Expression pattern of the mouse ortholog of the Pendred's syndrome gene (Pds) suggests a key role for pendrin in the inner ear. Proc Natl Acad Sci U S A. 1999; 96:9727–9732. [PubMed: 10449762]

Gray MA. Bicarbonate secretion: it takes two to tango. Nat Cell Biol. 2004; 6:292–294. [PubMed: 15057243]

Gray MA, Harris A, Coleman L, Greenwell JR, Argent BE. Two types of chloride channel on duct cells cultured from human fetal pancreas. Am J Physiol. 1989; 257:C240–C251. [PubMed: 2475028]

Grubb BR, Boucher RC. Pathophysiology of gene-targeted mouse models for cystic fibrosis. Physiol Rev. 1999; 79:S193–S214. [PubMed: 9922382]

Hughes GC, Post MJ, Simons M, Annex BH. Translational physiology: porcine models of human coronary artery disease: implications for preclinical trials of therapeutic angiogenesis. J Appl Physiol. 2003; 94:1689–1701. [PubMed: 12679343]

Klein I, Danzi S. Thyroid disease and the heart. Circulation. 2007; 116:1725–1735. [PubMed: 17923583]

Kleyman TR, Carattino MD, Hughey RP. ENaC at the cutting edge: regulation of epithelial sodium channels by proteases. J Biol Chem. 2009; 284:20447–20451. [PubMed: 19401469]

Ko SB, Zeng W, Dorwart MR, Luo X, Kim KH, Millen L, Goto H, Naruse S, Soyombo A, Thomas PJ, Muallem S. Gating of CFTR by the STAS domain of SLC26 transporters. Nat Cell Biol. 2004; 6:343–350. [PubMed: 15048129]

LeSimple P, Liao J, Robert R, Gruenert DC, Hanrahan JW. Cystic fibrosis transmembrane conductance regulator trafficking modulates the barrier function of airway epithelial cell monolayers. J Physiol. 2010; 588:1195–1209. [PubMed: 20156845]

Levy O, De la Vieja A, Ginter CS, Riedel C, Dai G, Carrasco N. N-linked glycosylation of the thyroid Na+/I− symporter (NIS). Implications for its secondary structure model. J Biol Chem. 1998; 273:22657–22663. [PubMed: 9712895]

Liu Y, Wang Y, Jiang Y, Zhu N, Liang H, Xu L, Feng X, Yang H, Ma T. Mild processing defect of porcine DeltaF508-CFTR suggests that DeltaF508 pigs may not develop cystic fibrosis disease. Biochem Biophys Res Commun. 2008; 373:113–118. [PubMed: 18555011]

Liu YY, Brent GA. Thyroid hormone crosstalk with nuclear receptor signaling in metabolic regulation. Trends Endocrinol Metab. 2010; 21:166–173. [PubMed: 20015660]

Madoff L. Elevated sweat chlorides and hypothyroidism. J Pediatr. 1968; 73:244–246. [PubMed: 4174554]

Mall M, Grubb BR, Harkema JR, O'Neal WK, Boucher RC. Increased airway epithelial Na+ absorption produces cystic fibrosis-like lung disease in mice. Nat Med. 2004; 10:487–493. [PubMed: 15077107]

Masilamani S, Kim GH, Mitchell C, Wade JB, Knepper MA. Aldosterone-mediated regulation of ENaC alpha, beta, and gamma subunit proteins in rat kidney. J Clin Invest. 1999; 104:R19–R23. [PubMed: 10510339]

Nilsson M, Bjorkman U, Ekholm R, Ericson LE. Iodide transport in primary cultured thyroid follicle cells: evidence of a TSH-regulated channel mediating iodide efflux selectively across the apical domain of the plasma membrane. Eur J Cell Biol. 1990; 52:270–281. [PubMed: 1706997]

Nilsson M, Bjorkman U, Ekholm R, Ericson LE. Polarized efflux of iodide in porcine thyrocytes occurs via a cAMP-regulated iodide channel in the apical plasma membrane. Acta Endocrinol (Copenh). 1992; 126:67–74. [PubMed: 1371033]

Ostedgaard LS, Rogers CS, Dong Q, Randak CO, Vermeer DW, Rokhlina T, Karp PH, Welsh MJ. Processing and function of CFTR-DeltaF508 are species-dependent. Proc Natl Acad Sci U S A. 2007; 104:15370–15375. [PubMed: 17873061]

Panesar NS. Could growth retardation in cystic fibrosis be partly due to deficient steroid and thyroid hormonogenesis? Med Hypotheses. 1999; 53:530–532. [PubMed: 10687897]

Pearson J, Bourke JR, Manley SW, Huxham GJ, Matainaho T, Gerard C, Verrier B, Mauchamp J. Electrophysiological correlates of fluid transport in cultured porcine thyroid cells. J Endocrinol. 1988; 119:309–314. [PubMed: 2462003]

Peirson SN, Butler JN, Foster RG. Experimental validation of novel and conventional approaches to quantitative real-time PCR data analysis. Nucleic Acids Res. 2003; 31:e73. [PubMed: 12853650]

Penel C, Gerard C, Mauchamp J, Verrier B. The thyroid cell monolayer in culture. A tight sodium absorbing epithelium. Pflugers Arch. 1989; 414:509–515. [PubMed: 2550888]

Price MP, Ishihara H, Sheppard DN, Welsh MJ. Function of Xenopus cystic fibrosis transmembrane conductance regulator (CFTR) Cl channels and use of human-Xenopus chimeras to investigate the pore properties of CFTR. J Biol Chem. 1996; 271:25184–25191. [PubMed: 8810276]

Qiu W, Laheri A, Leung S, Guggino SE. Hormones increase mRNA of cyclic-nucleotide-gated cation channels in airway epithelia. Pflugers Arch. 2000; 441:69–77. [PubMed: 11205064]

Reddy MM, Light MJ, Quinton PM. Activation of the epithelial Na+ channel (ENaC) requires CFTR Cl- channel function. Nature. 1999; 402:301–304. [PubMed: 10580502]

Riordan JR, Rommens JM, Kerem B, Alon N, Rozmahel R, Grzelczak Z, Zielenski J, Lok S, Plavsic N, Chou JL, et al. Identification of the cystic fibrosis gene: cloning and characterization of complementary DNA. Science. 1989; 245:1066–1073. [PubMed: 2475911]

Rochelle LG, Li DC, Ye H, Lee E, Talbot CR, Boucher RC. Distribution of ion transport mRNAs throughout murine nose and lung. Am J Physiol Lung Cell Mol Physiol. 2000; 279:L14–L24. [PubMed: 10893198]

Rogers CS, Hao Y, Rokhlina T, Samuel M, Stoltz DA, Li Y, Petroff E, Vermeer DW, Kabel AC, Yan Z, Spate L, Wax D, Murphy CN, Rieke A, Whitworth K, Linville ML, Korte SW, Engelhardt JF, Welsh MJ, Prather RS. Production of CFTR-null and CFTR-DeltaF508 heterozygous pigs by adeno-associated virus-mediated gene targeting and somatic cell nuclear transfer. J Clin Invest. 2008a; 118:1571–1577. [PubMed: 18324337]

Rogers CS, Stoltz DA, Meyerholz DK, Ostedgaard LS, Rokhlina T, Taft PJ, Rogan MP, Pezzulo AA, Karp PH, Itani OA, Kabel AC, Wohlford-Lenane CL, Davis GJ, Hanfland RA, Smith TL, Samuel M, Wax D, Murphy CN, Rieke A, Whitworth K, Uc A, Starner TD, Brogden KA, Shilyansky J, McCray PB Jr, Zabner J, Prather RS, Welsh MJ. Disruption of the CFTR gene produces a model of cystic fibrosis in newborn pigs. Science. 2008b; 321:1837–1841. [PubMed: 18818360]

Royaux IE, Suzuki K, Mori A, Katoh R, Everett LA, Kohn LD, Green ED. Pendrin, the protein encoded by the Pendred syndrome gene (PDS), is an apical porter of iodide in the thyroid and is regulated by thyroglobulin in FRTL-5 cells. Endocrinology. 2000; 141:839–845. [PubMed: 10650967]

Scholte BJ, Colledge WH, Wilke M, de Jonge H. Cellular and animal models of cystic fibrosis, tools for drug discovery. Drug Discov Today Dis Models. 2006; 3:251–259.

Schwiebert EM, Benos DJ, Egan ME, Stutts MJ, Guggino WB. CFTR is a conductance regulator as well as a chloride channel. Physiol Rev. 1999; 79:S145–S166. [PubMed: 9922379]

Scott DA, Wang R, Kreman TM, Sheffield VC, Karniski LP. The Pendred syndrome gene encodes a chloride-iodide transport protein. Nat Genet. 1999; 21:440–443. [PubMed: 10192399]

Shcheynikov N, Yang D, Wang Y, Zeng W, Karniski LP, So I, Wall SM, Muallem S. The Slc26a4 transporter functions as an electroneutral Cl-/I-/HCO3- exchanger: role of Slc26a4 and Slc26a6 in I- and HCO3- secretion and in regulation of CFTR in the parotid duct. J Physiol. 2008; 586:3813–3824. [PubMed: 18565999]

Sheppard DN, Welsh MJ. Structure and function of the CFTR chloride channel. Physiol Rev. 1999; 79:S23–S45. [PubMed: 9922375]

Stoltz DA, Meyerholz DK, Pezzulo AA, Ramachandran S, Rogan MP, Davis GJ, Hanfland RA, Wohlford-Lenane C, Dohrn CL, Bartlett JA, Nelson GAt, Chang EH, Taft PJ, Ludwig PS, Estin M, Hornick EE, Launspach JL, Samuel M, Rokhlina T, Karp PH, Ostedgaard LS, Uc A, Starner TD, Horswill AR, Brogden KA, Prather RS, Richter SS, Shilyansky J, McCray PB Jr, Zabner J, Welsh MJ. Cystic fibrosis pigs develop lung disease and exhibit defective bacterial eradication at birth. Sci Transl Med. 2010; 2 29ra31.

Tabcharani JA, Chang XB, Riordan JR, Hanrahan JW. The cystic fibrosis transmembrane conductance regulator chloride channel. Iodide block and permeation. Biophys J. 1992; 62:1–4. [PubMed: 1376160]

Tabcharani JA, Linsdell P, Hanrahan JW. Halide permeation in wild-type and mutant cystic fibrosis transmembrane conductance regulator chloride channels. J Gen Physiol. 1997; 110:341–354. [PubMed: 9379167]

Tedelind S, Larsson F, Johanson C, van Beeren HC, Wiersinga WM, Nystrom E, Nilsson M. Amiodarone inhibits thyroidal iodide transport in vitro by a cyclic adenosine 5'-monophosphate- and iodine-independent mechanism. Endocrinology. 2006; 147:2936–2943. [PubMed: 16527845]

van den Hove MF, Croizet-Berger K, Jouret F, Guggino SE, Guggino WB, Devuyst O, Courtoy PJ. The loss of the chloride channel, ClC-5, delays apical iodide efflux and induces a euthyroid goiter in the mouse thyroid gland. Endocrinology. 2006; 147:1287–1296. [PubMed: 16306076]

Verrier B, Champigny G, Barbry P, Gerard C, Mauchamp J, Lazdunski M. Identification and properties of a novel type of Na+-permeable amiloride-sensitive channel in thyroid cells. Eur J Biochem. 1989; 183:499–505. [PubMed: 2550220]

Wangemann P, Kim HM, Billings S, Nakaya K, Li X, Singh R, Sharlin DS, Forrest D, Marcus DC, Fong P. Developmental delays consistent with cochlear hypothyroidism contribute to failure to develop hearing in mice lacking Slc26a4/pendrin expression. Am J Physiol Renal Physiol. 2009; 297:F1435–F1447. [PubMed: 19692489]

Welsh, MJ.; Ramsey, BW.; Accurso, F.; Cutting, G. Cystic Fibrosis. In: Scriver, Cr; Beaudet, AL.; Sly, WS.; Valle, D., editors. Metabolic and Molecular Basis of Inherited Diseas. New York: McGraw-Hill; 2001. p. 5121-5188.

Williams DW, Wynford-Thomas D. Human thyroid epithelial cells. Methods Mol Biol. 1997; 75:163–172. [PubMed: 9276268]

Yoshida A, Taniguchi S, Hisatome I, Royaux IE, Green ED, Kohn LD, Suzuki K. Pendrin is an iodide-specific apical porter responsible for iodide efflux from thyroid cells. J Clin Endocrinol Metab. 2002; 87:3356–3361. [PubMed: 12107249]

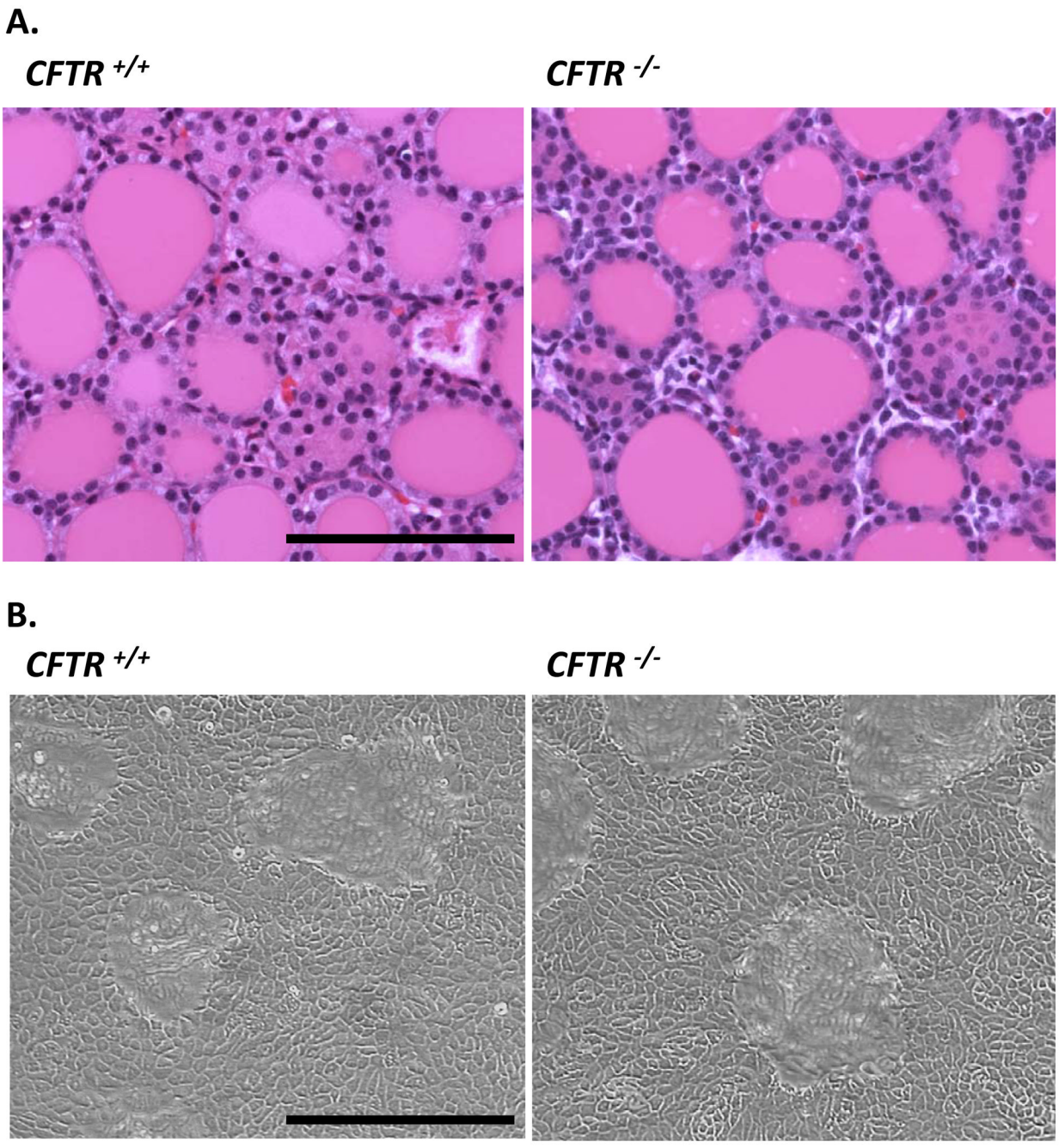

Figure 1.
A) Histology and **B**) growth of litter-matched, 1-day-old *CFTR* $^{+/+}$ and *CFTR* $^{-/-}$ pig thyroids. Both image sets were taken at the same magnification; scale bar, 100 μm. **A**) HE staining of paraffin sections prepared from litter-matched, neonatal pig thyroids. **B**) Phase image of pThEC cultures after 1 week of growth.

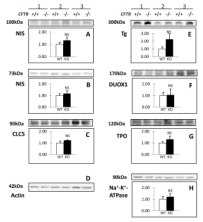

Figure 2.

Expression of thyroid-specific proteins by *CFTR* $^{+/+}$ and *CFTR* $^{-/-}$ pThECs. Cultures were prepared from three separate litter-matched pairs. The normalized expression levels of the two forms of NIS are shown in panels **A**) and **B**); neither form was expressed differently (p = 0.32 for the 100 kDa form and 0.19 for the 73 kDa species. Panel **C**) ClC-5 expression likewise did not differ between the *CFTR* $^{+/+}$ and *CFTR* $^{-/-}$ pThECs (p = 0.40). Panels **E)**, **F)** and **G)** summarize relative levels of thyroglobulin (Tg), DUOX1 and thyroperoxidase (TPO), all which did not reveal significant differences (p = 0.09, 0.82 and 0.47, respectively). **H**) Expression of the Na^+/K^+ ATPase was obtained as an approximate index of transport capacity; no difference between the two groups was found. All measurements were obtained by normalization to the respective actin signal (**D**). All p values were obtained using paired t-tests.

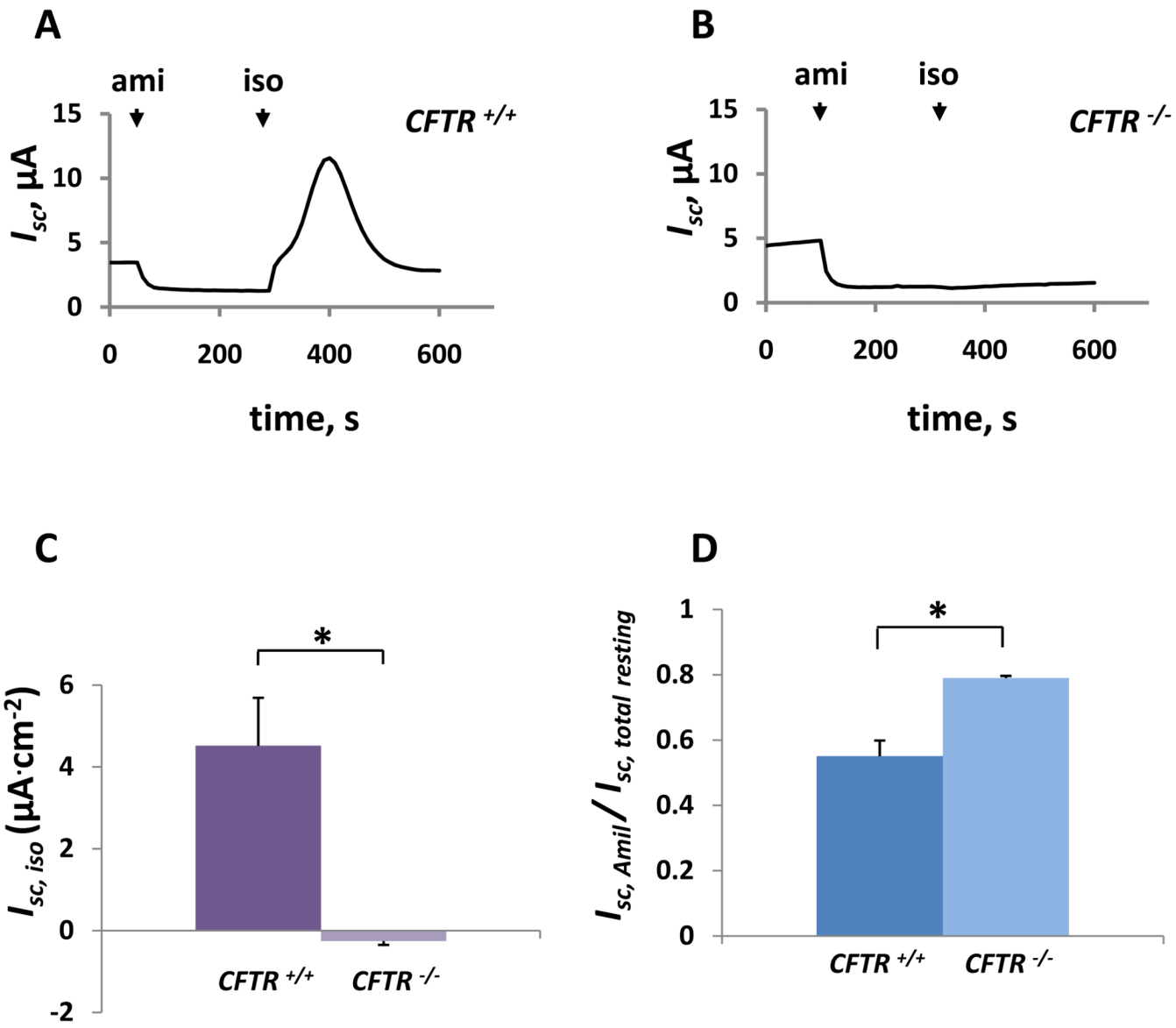

Figure 3.

I_{sc} recordings show the presence of isoproterenol-activated I_{sc} in **A)** *CFTR* $^{+/+}$, but not **B)** *CFTR* $^{-/-}$ pThECs. Addition of isoproterenol is indicated by arrow labeled "iso". Note that the baseline I_{sc} is inhibited swiftly by addition of mucosal amiloride (10^{-5} M; "amil") to both wild type and knockout monolayers. The traces are responses of monolayers grown from 1-day-old littermates and studied at day 14 post-plating. Baseline I_{sc} values were 3.45 µA.cm^2 and 4.705 µA.cm^2 for this pair of *CFTR* $^{+/+}$ and *CFTR* $^{-/-}$ pThEC monolayers, respectively. The amiloride-sensitive fraction of I_{sc} for the *CFTR* $^{+/+}$ pThEC monolayer depicted here was 0.63. For the *CFTR* $^{-/-}$ trace shown, this was 0.74. **C)** Summarized peak responses to serosal isoproterenol (10^{-5} M) are shown for *CFTR* $^{+/+}$ pThEC monolayers (*left*; n = 9 monolayers from 5 preparations). For comparison, data from *CFTR* $^{-/-}$ pThECs are provided (*right*; n = 5 monolayers from 3 preparations). **D)** Fractional amiloride-sensitive I_{sc} is significantly greater in pThECs grown from *CFTR* $^{-/-}$ thyroids (0.79 ± 0.007; *right*) compared to that measured in *CFTR* $^{+/+}$ thyroid-derived monolayers (0.55 ± 0.048; *left*). Data represent the mean values ± SEM.

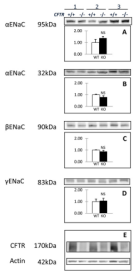

Figure 4.
Quantitative immunoblot analysis shows that *CFTR* $^{+/+}$ and *CFTR* $^{-/-}$ pThECs express ENaC subunit proteins at similar levels. **A)** Relative levels of the α-ENaC 95 kDa and **B)** 32 kDa species were not altered in *CFTR* $^{-/-}$ cells compared *CFTR* $^{+/+}$ ($p = 0.44$ and 0.30, respectively). This was similarly the case for **C)** β-ENaC ($p = 0.28$) and **D)** γ-ENaC (83 kDa) ($p = 0.70$). Panel **E)** depicts the corresponding control probes for CFTR and actin. All p values were obtained using paired t-tests on n = 3 litter-matched pairs.

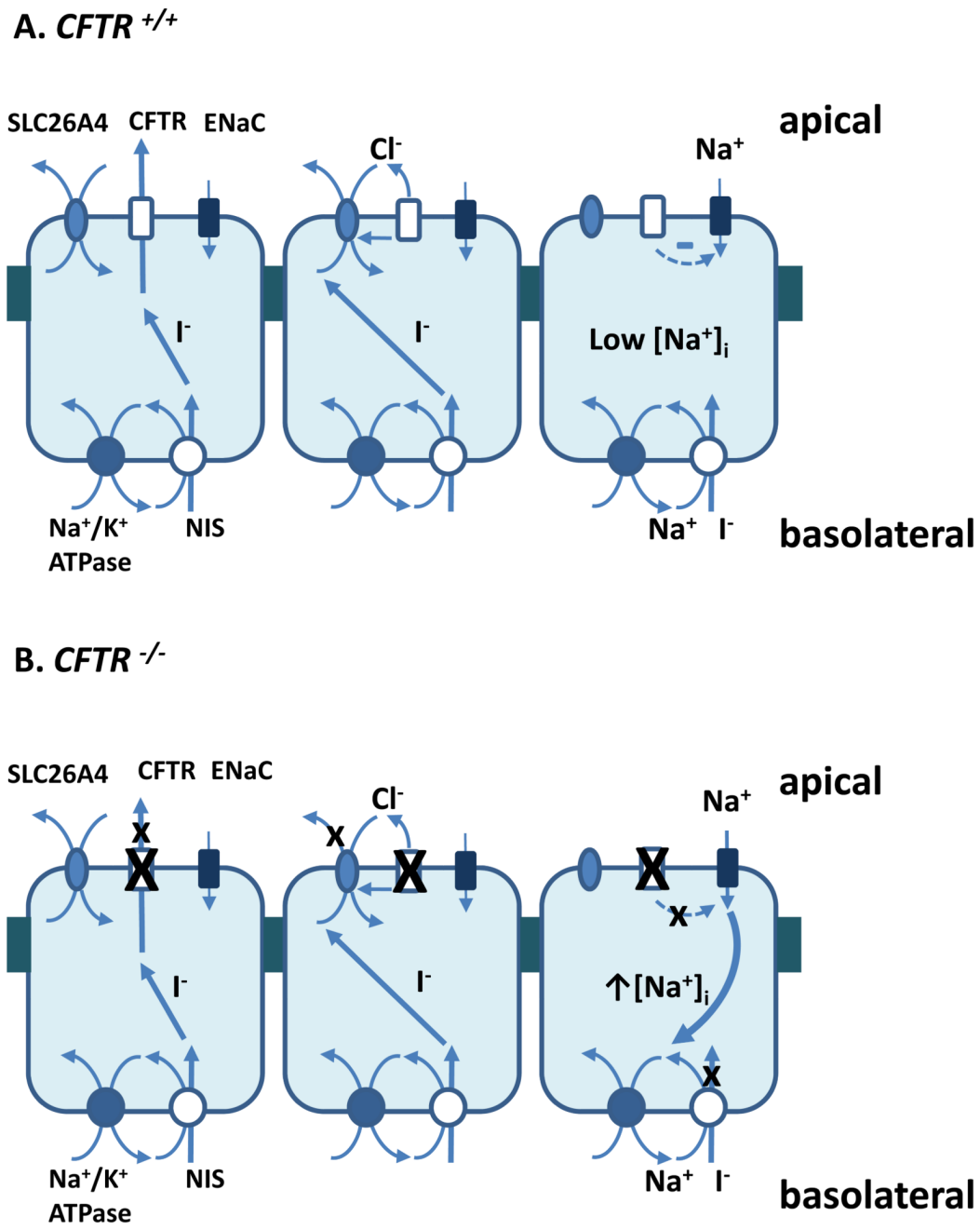

Figure 5.

Hypothetical models linking CFTR function to thyroid hormonogenesis are shown in this schematic diagram. ***Panel A*** shows hypothesized CFTR functions. *Leftmost diagram* depicts the situation in which CFTR directly conducts I^-. *Middle diagram* shows CFTR regulates SLC26A4/Pendrin-mediated I^- movement, possibly by STAS domain interactions and transport of counter-anions for SLC26A4. *Right diagram* shows the situation whereby CFTR regulates Na^+ entry through ENaC, thereby preserving the Na^+ gradient that is required for NIS-mediated I^- uptake. ***Panel B*** illustrates predicted outcomes of *CFTR* ablation, based on each of the schemes illustrated in ***Panel A***.

Table 1

Primers used in qRT-PCR reactions

Gene	Forward Primer Sequence, 5' → 3'	Reverse Primer Sequence, 5' → 3'	Product Size, bp	GenBank No.
CFTR	CCGGGCACCATTAAAGAAAAC	GCCATCAATTTACAGACACAGC	293	AY585334.1
SLC26A4	ATCTACGGAGCCAGGTGAAATC	GAAATAACGCCTAGCAATAATCTTAG	372	DQ141305.1
CLCN5	GAAATAACGCCTAGCAATAATCTTAG	CGCGGGAGTCCCAAAGAC	360	NM_214139.1
SLC5A5	CTCTCCTGGCAGGGCATATCT	GCTGAGGGTGCCGCTGTA	125	NM_214410.1
SCNN1A	CCCCATCCGCCTGGTGTGCT	GGAAGAGGAGCTTGTCCGAGTTGA	157	AY394432
SCNN1B	TGCTGTGCCTCATCGAGTTTG	TGCAGACGCAGGGAGTCATAGTTG	277	NM_000336.2
SCNN1G	TCAAGAAGAATCTGCCCGTGA	GGAAGTGGACTTTGATGGAAACTG	237	X87160.1
CNGA1	TTTGACTATCTGTGGACCAA	CAAGTTTGCCTTCTTTGATA	262	BGISUST0000897216[1]
18S	GTAACCCGTTGAACCCCATT	CCATCCAATCGGTAGTAGCG	147	NR_003286.2

[1]Gene information is from Pig Genomic Informatics System (PigGIS; http://pig.genomics.org.cn/).

Table 2

qRT-PCR data summary: pThEC cell expression of genes encoding transport proteins

Gene	*n*(pairs)	Mean C_t[1], *CFTR*$^{+/+}$	Mean C_t, *CFTR*$^{-/-}$	Mean R_0[2], *CFTR*$^{+/+}$	Mean R_0, *CFTR*$^{-/-}$	Fold change[3], *CFTR*$^{-/-}$ / *CFTR*$^{+/+}$
CFTR	5	23.48 ± 0.29	N/A	3.94E-05 ± 1.11E-05	N/A	N/A
SLC26A4	3	>35[4]	>35[4]	N/A	N/A	N/A
CLCN5	3	27.73 ± 0.32	27.62 ± 0.33	2.61E-06 ± 4.98E-07	2.48E-06 ± 6.11E-07	0.96 ± 0.19
SLC5A5	5	27.88 ± 0.54	27.18 ± 0.60	1.95E-06 ± 4.15E-07	1.84E-06 ± 4.45E-07	0.99 ± 0.15
SCNN1A	5	24.41 ± 0.29	24.26 ± 0.26	1.15E-05 ± 3.65E-06	9.48E-06 ± 1.75E-06	1.28 ± 0.21
SCNN1B	5	27.07 ± 0.55	27.15 ± 0.41	2.09E-06 ± 7.04E-07	1.89E-06 ± 4.38E-06	0.90 ± 0.08
SCNN1G	5	27.97 ± 0.39	27.8 ± 0.42	1.14E-06 ± 4.36E-07	1.31E-06 ± 3.85E-07	1.06 ± 0.15
CNGA1	3	34.03 ± 0.24	33.56 ± 0.67	2.47E-08 ± 3.11E-09	3.51E-08 ± 1.69E-08	1.61 ± 0.93

N/A: not applicable

n is the number of litter-matched cultures

[1] Mean C_t values ± SEM

[2] Mean R_0 values ± SEM; R_0, initial reporter fluorescence normalized to that of 18S rRNA

[3] Values are means ± SEM for the fold-change (*CFTR* $^{-/-}$/*CFTR*$^{+/+}$) of normalized R_0

[4] C_t value for SLC26A4 is larger than 35 and hence not reliably detected.